

Spectral flow of vortex shape modes over the BPS 2-vortex moduli space

A. Alonso Izquierdo ^a, W. Garcia Fuertes ^b, N.S. Manton ^c
and J. Mateos Guilarte ^d

^a*Departamento de Matematica Aplicada, Universidad de Salamanca, Salamanca, Spain*

^b*Departamento de Fisica, Universidad de Oviedo, Oviedo, Spain*

^c*Department of Applied Mathematics and Theoretical Physics, University of Cambridge, Cambridge, U.K.*

^d*Departamento de Fisica Fundamental, Universidad de Salamanca, Salamanca, Spain*

E-mail: alonsoiz@usal.es, wifredo@uniovi.es, nsm10@cam.ac.uk,
guilarte@usal.es

ABSTRACT: The flow of shape eigenmodes of the small fluctuation operator around BPS 2-vortex solutions is calculated, as a function of the intervortex separation $2d$. For the rotationally-invariant 2-vortex, with $d = 0$, there are three discrete modes; the lowest is non-degenerate and the upper two are degenerate. As d increases, the degeneracy splits, with one eigenvalue increasing and entering the continuous spectrum, and the other decreasing and asymptotically coalescing with the lowest eigenvalue, where they jointly become the eigenvalue of the 1-vortex radial shape mode. The behaviour of the eigenvalues near $d = 0$ is clarified using a perturbative analysis, and also in light of the 2-vortex moduli space geometry.

KEYWORDS: Spontaneous Symmetry Breaking, Topological States of Matter

ARXIV EPRINT: [2310.17486](https://arxiv.org/abs/2310.17486)

Contents

1	Introduction	1
2	BPS vortices in the Abelian Higgs model: SUSY structure of the fluctuation operator	2
3	The spectrum of the BPS 2-vortex fluctuation operator	4
4	Perturbation theory near $d = 0$	9
5	Insight from the 2-vortex moduli space	10
6	Outlook	12

1 Introduction

Collective coordinate dynamics has been successfully implemented in [1] to describe the low-energy effective theory governing collisions between ϕ^4 -kinks. The collective coordinates associated to each kink consist of the kink center a and the amplitude A of the unique shape mode of kink fluctuations. The reduced system in the centre of mass frame, assuming reflection symmetry, has a two-dimensional Lagrangian with a kinetic energy involving a metric depending on A and a potential energy also depending on A .

It seems feasible to develop a similar effective theory for BPS n -vortex dynamics in the Abelian Higgs model at critical coupling. For a 1-vortex, the collective coordinates would be the vortex center and the amplitude of the unique discrete fluctuation mode — the radial shape mode. Finding a collective coordinate treatment in the case of 2-vortices would be far more interesting. Here, the discrete eigenvalues and eigenfunctions of the second-order fluctuation operator vary with the separation of the 1-vortex constituents. Internal shape modes of vortices of various kinds have been studied, e.g., in refs. [2–5], but so far, almost exclusively for coincident-vortex solutions.

The moduli space of BPS n -vortices is the space of sets of n unordered points in the plane — the points where the Higgs field vanishes. This is a non-singular complex manifold [6–8], even where vortices coincide, but one needs to be careful about the choice of coordinates. In particular, for 2-vortices with fixed centre of mass at the origin, if the constituent vortices have a separation $2d$, then it is d^2 rather than d that is a good radial coordinate on the moduli space.

For each $n > 0$ there is a unique n -vortex, rotationally-invariant around the origin, for which the n constituent vortex locations coincide. The spectral problem of the second-order vortex fluctuation operator in this case resembles that of the planar Hydrogen atom, but the potential well is bounded from below and reaches the continuous-spectrum threshold exponentially fast as the radius increases, which implies that there exist at most a finite number of discrete shape modes. In [2], these facts guided the search for discrete modes.

It was found, for example, that for $n = 1$ there is only one discrete shape mode whereas for $n = 2$ there are three.

The generic BPS 2-vortex is formed from two 1-vortices separated by an arbitrary finite distance. The spectrum of vortex fluctuations is then akin to the quantum spectrum of a particle moving in the field created by two centers of force, where the centers are freely movable. In this paper we investigate how the shape modes and their eigenfrequencies vary with the vortex separation. The number of discrete modes remains finite, and in fact decreases from three to two as the separation increases.

Our results should lead to a generalisation of the notion of geodesic flow on the 2-vortex moduli space as an approximation to 2-vortex dynamics. Allowing for the possibility of excited shape modes will require a more complicated collective coordinate model for the low-energy dynamics of vortices, including a potential on the moduli space. If the vortex motion is slow, and the evolution of the shape mode amplitudes is treated adiabatically, then a Berry connection will probably also be needed.

2 BPS vortices in the Abelian Higgs model: SUSY structure of the fluctuation operator

We start from the action of the relativistic Abelian Higgs model, describing the minimal coupling between a U(1) gauge field and a charged scalar field in a phase where the gauge symmetry is broken spontaneously. We focus on the BPS critical value of the coupling (the strength of the Higgs potential) where the Higgs and gauge field masses are equal [9, 10]. In terms of non-dimensional coordinates, couplings and fields, the action functional for this system is

$$S[\phi, A] = \int dx_0 dx_1 dx_2 \left[-\frac{1}{4} F_{\mu\nu} F^{\mu\nu} + \frac{1}{2} \overline{D_\mu \phi} D^\mu \phi - \frac{1}{8} (\overline{\phi} \phi - 1)^2 \right]. \quad (2.1)$$

The ingredients here are a complex scalar (Higgs) field $\phi(x) = \phi_1(x) + i\phi_2(x)$, a U(1) gauge potential $A_\mu(x) = (A_0(x), A_1(x), A_2(x))$, the covariant derivative $D_\mu \phi(x) = (\partial_\mu - iA_\mu(x))\phi(x)$ and the electromagnetic field tensor $F_{\mu\nu}(x) = \partial_\mu A_\nu(x) - \partial_\nu A_\mu(x)$. Our Minkowski-space metric tensor is $g_{\mu\nu} = \text{diag}(1, -1, -1)$, with $\mu, \nu = 0, 1, 2$, and we use the Einstein summation convention. In the temporal gauge $A_0 = 0$, the energy of static field configurations becomes

$$V[\phi, A] = \int_{\mathbb{R}^2} d^2x \left[\frac{1}{2} F_{12}^2 + \frac{1}{2} \overline{D_1 \phi} D_1 \phi + \frac{1}{2} \overline{D_2 \phi} D_2 \phi + \frac{1}{8} (\overline{\phi} \phi - 1)^2 \right]. \quad (2.2)$$

We interchangeably use Cartesian and polar coordinates $\vec{x} = (x_1, x_2) = (x, y) = (r \cos \theta, r \sin \theta)$ with $d^2x = dx dy$. The energy (2.2), treated non-relativistically, models the free energy of a superconducting material arising in the Ginzburg-Landau theory of superconductivity — see formula (17) in [11] where the order parameter $|\phi|^2 = \overline{\phi} \phi$ corresponds to the density of Cooper pairs.

Critical points of $V[\phi, A]$ that satisfy the boundary conditions

$$\overline{\phi} \phi|_{S_\infty^1} = 1, \quad D_i \phi|_{S_\infty^1} = 0 \quad \text{and} \quad F_{12}|_{S_\infty^1} = 0 \quad (2.3)$$

on the circle at infinity S_∞^1 (i.e. as $r \rightarrow \infty$) have finite energy. Indeed, it can be checked that the configuration space of static fields,

$$\mathcal{C} = \{\{\phi, A\} \text{ s.t. } V[\phi, A] < \infty\} = \sqcup_{n \in \mathbb{Z}} \mathcal{C}_n, \quad (2.4)$$

is the union of \mathbb{Z} topologically disconnected sectors. Here, n is the vorticity or winding number of the map $\phi|_\infty : S_\infty^1 \rightarrow S^1$ from the circle at infinity to the vacuum orbit $|\phi|^2 = 1$, parametrised by the phase of ϕ . It follows from the vanishing of the covariant derivative of ϕ at infinity, that n is also the normalised magnetic flux, $\Phi \equiv \frac{1}{2\pi} \int_{\mathbb{R}^2} d^2x F_{12} = n$. In the BPS regime, $V[\phi, A]$ can be written in the form, see [9],

$$V[\phi, A] = \frac{1}{2} \int_{\mathbb{R}^2} d^2x \left[\left(F_{12} \pm \frac{1}{2} (\bar{\phi} \phi - 1) \right)^2 + |D_1 \phi \pm i D_2 \phi|^2 \right] \pm \frac{1}{2} \int_{\mathbb{R}^2} d^2x F_{12}, \quad (2.5)$$

which implies that BPS vortices are solutions of the first-order PDEs

$$D_1 \phi \pm i D_2 \phi = 0, \quad F_{12} \pm \frac{1}{2} (\bar{\phi} \phi - 1) = 0, \quad (2.6)$$

and are absolute minima of the energy for each n , with $V[\phi, A] = \pi|n|$. For n positive, the upper signs in (2.6) need to be chosen. Then, given n , there exist BPS vortex solutions characterized by n arbitrary locations (points) in the plane, which are the zeros of the scalar field counted with multiplicity, and simultaneously the locations of maximal magnetic field. n -vortex solutions therefore have $2n$ real moduli. For the sake of clarity in later formulas we shall denote the scalar field profile $\phi(\vec{x})$ of an n -vortex solution as $\psi^{(n)}(\vec{x}) = \psi_1^{(n)}(\vec{x}) + i \psi_2^{(n)}(\vec{x})$ and the gauge (vector) potential $A_k(\vec{x})$ as $V_k^{(n)}(\vec{x})$. The main theme of this paper is the construction of field fluctuations around 2-vortices $\{\psi^{(2)}(\vec{x}), V_k^{(2)}(\vec{x})\}$, and analysis of how they depend on the vortex separation.

To find the linear fluctuation modes, we consider the evolution of small perturbations $\varphi_j(\vec{x})$ and $a_k(\vec{x})$ around BPS vortex fields $\psi_j^{(n)}(\vec{x})$ and $V_k^{(n)}(\vec{x})$. The total fields are

$$\phi_j(\vec{x}) = \psi_j^{(n)}(\vec{x}) + \epsilon \varphi_j(\vec{x}) e^{i\omega t}, \quad A_k(\vec{x}) = V_k^{(n)}(\vec{x}) + \epsilon a_k(\vec{x}) e^{i\omega t} \quad (2.7)$$

with ϵ small, and they still belong to the n -vortex topological sector. To discard pure gauge fluctuations, we impose the *background gauge*

$$B(\varphi_j, a_k) = \partial_k a_k(\vec{x}) - (\psi_1^{(n)}(\vec{x}) \varphi_2(\vec{x}) - \psi_2^{(n)}(\vec{x}) \varphi_1(\vec{x})) = 0 \quad (2.8)$$

as the gauge fixing condition on the perturbations. Substituting (2.7) into the field equations and linearizing, the eigenfrequencies ω and eigenmodes

$$\xi(\vec{x}) = \left(a_1(\vec{x}), a_2(\vec{x}), \varphi_1(\vec{x}), \varphi_2(\vec{x}) \right)^t \quad (2.9)$$

are found to be solutions of the spectral problem $\mathcal{H}^+ \xi_\lambda(\vec{x}) = \omega_\lambda^2 \xi_\lambda(\vec{x})$, see [12–14]. Here, λ is a label in either the discrete or continuous spectrum, and \mathcal{H}^+ is the second-order vortex fluctuation operator

$$\mathcal{H}^+ = \begin{pmatrix} -\nabla^2 + |\psi|^2 & 0 & -2D_1 \psi_2 & 2D_1 \psi_1 \\ 0 & -\nabla^2 + |\psi|^2 & -2D_2 \psi_2 & 2D_2 \psi_1 \\ -2D_1 \psi_2 & -2D_2 \psi_2 & -\nabla^2 + \frac{1}{2}(3|\psi|^2 - 1) + V_k V_k & -2V_k \partial_k - \partial_k V_k \\ 2D_1 \psi_1 & 2D_2 \psi_1 & 2V_k \partial_k + \partial_k V_k & -\nabla^2 + \frac{1}{2}(3|\psi|^2 - 1) + V_k V_k \end{pmatrix} \quad (2.10)$$

where $|\psi|^2 = \psi_1^2 + \psi_2^2$, and $\{\psi, V_k\}$ satisfy eqs. (2.6). The fluctuation vectors $\xi(\vec{x})$ belong in general to a rigged Hilbert space. There are square integrable eigenfunctions $\xi_\lambda(\vec{x}) \in L^2(\mathbb{R}^2) \otimes \mathbb{R}^4$ belonging to the discrete spectrum, for which the squared norm $\|\xi_\lambda(\vec{x})\|^2 = \int_{\mathbb{R}^2} d^2x [(a_1(\vec{x}))^2 + (a_2(\vec{x}))^2 + (\varphi_1(\vec{x}))^2 + (\varphi_2(\vec{x}))^2]$ is bounded, as well as continuous spectrum eigenfunctions.

Weinberg [15] proved that there are $2n$ linearly-independent normalizable zero modes (having eigenvalues $\omega^2 = 0$) for any BPS n -vortex solution. These can be characterized as lying in the kernel of the operator

$$\mathcal{D} = \begin{pmatrix} -\partial_2 & \partial_1 & \psi_1 & \psi_2 \\ -\partial_1 & -\partial_2 & -\psi_2 & \psi_1 \\ \psi_1 & -\psi_2 & -\partial_2 + V_1 & -\partial_1 - V_2 \\ \psi_2 & \psi_1 & \partial_1 + V_2 & -\partial_2 + V_1 \end{pmatrix}. \quad (2.11)$$

Analysis of these zero modes was further developed in [16] and [17], motivated by the study of vortex scattering at low energies within the approach of geodesic dynamics in the n -vortex moduli space, see e.g. [18].

A crucial point for the calculations in this paper is that

$$\mathcal{H}^+ = \mathcal{D}^\dagger \mathcal{D} \quad \text{and} \quad \mathcal{H}^- = \mathcal{D} \mathcal{D}^\dagger \quad (2.12)$$

are SUSY (supersymmetry) partners, and therefore isospectral in the strictly positive part of the spectrum. Moreover,

$$\mathcal{H}^- = \begin{pmatrix} -\nabla^2 + |\psi|^2 & 0 & 0 & 0 \\ 0 & -\nabla^2 + |\psi|^2 & 0 & 0 \\ 0 & 0 & -\nabla^2 + \frac{1}{2}(|\psi|^2 + 1) + V_k V_k & -2V_k \partial_k - \partial_k V_k \\ 0 & 0 & 2V_k \partial_k + \partial_k V_k & -\nabla^2 + \frac{1}{2}(|\psi|^2 + 1) + V_k V_k \end{pmatrix} \quad (2.13)$$

is a simpler operator than \mathcal{H}^+ , and its spectrum is easier to investigate. For \mathcal{H}^- , it was proved in [2, 3] that it is sufficient to find eigenfunctions of the form $\xi_\lambda^-(\vec{x}) = (a_1(\vec{x}), 0, 0, 0)^t$, satisfying

$$(-\nabla^2 + |\psi^{(n)}(\vec{x})|^2) a_1(\vec{x}) = \omega_\lambda^2 a_1(\vec{x}). \quad (2.14)$$

The corresponding eigenfunction of the SUSY partner operator \mathcal{H}^+ , sharing the positive eigenvalue ω_λ^2 and the same normalization, is

$$\xi_\lambda^+(\vec{x}) = \frac{1}{\omega_\lambda} \mathcal{D}^\dagger \xi_\lambda^-(\vec{x}) = \frac{1}{\omega_\lambda} \left(\partial_2 a_1(\vec{x}), -\partial_1 a_1(\vec{x}), \psi_1(\vec{x}) a_1(\vec{x}), \psi_2(\vec{x}) a_1(\vec{x}) \right)^t. \quad (2.15)$$

3 The spectrum of the BPS 2-vortex fluctuation operator

In this section we obtain numerically the discrete, positive eigenvalues and eigenfunctions of the second-order fluctuation operator \mathcal{H}^+ evaluated at BPS 2-vortex solutions $\{\psi^{(2)}(\vec{x}), V_k^{(2)}(\vec{x})\}$. Recall that these 2-vortices can be interpreted as two separated 1-vortices. If the 2-vortex mass center is located at the origin, the 1-vortex locations (zeros of $\psi^{(2)}$) can be assumed to

be at $(d, 0)$ and $(-d, 0)$, with equivalent solutions being obtained by translation and rotation. The first task is to construct the 2-vortex solution with these zeros.

We start from the more general, rotationally-invariant n -vortex solution, having the polar coordinate form

$$\psi^{(n)}(\vec{x}) = f_n(r) e^{in\theta}, \quad rA_\theta^{(n)}(\vec{x}) = n\beta_n(r), \quad (3.1)$$

and with the radial gauge $A_r^{(n)} = 0$ imposed. The functions $f_n(r)$ and $\beta_n(r)$ need to satisfy the first-order coupled equations

$$\frac{df_n}{dr} = \frac{n}{r} f_n(r)[1 - \beta_n(r)], \quad \frac{d\beta_n}{dr} = \frac{r}{2n} [1 - f_n^2(r)], \quad (3.2)$$

and the asymptotic conditions $f_n(r) \rightarrow 1$ and $\beta_n(r) \rightarrow 1$ as $r \rightarrow \infty$. The requirement of regularity at the origin fixes the behaviour for small r to be $f_n(r) \sim d_n r^n$ and $\beta_n(r) \sim \frac{1}{4n} r^2$, where d_n is a constant depending on n . Using eqs. (3.2), the radial profiles $f_n(r)$ and $\beta_n(r)$ for $n = 1$ and $n = 2$ (and higher n) are easily generated. A 2-vortex whose zeros are well separated is then approximated by superposing two rotationally-invariant 1-vortices, translated to have the desired zeros. A 2-vortex with coincident zeros is the rotationally-invariant solution with radial profiles $f_2(r)$ and $\beta_2(r)$.

To construct 2-vortex solutions whose zeros are separated by an intermediate distance $2d$, we take advantage of the Bogomolny energy bound, which for 2-vortices is $V[\psi^{(2)}, V^{(2)}] = 2\pi$. Our strategy is to numerically construct an $n = 2$ configuration with zeros at $(d, 0)$ and $(-d, 0)$, that accurately saturates this bound. Indeed, the deviation of the energy from this bound is an estimate of the solution's precision. To generate initial data, we use a generalized $n = 1$ configuration centered at $(d, 0)$,

$$\begin{aligned} \phi^{(1)}(\vec{x}, d, \alpha) &= \left[\alpha f_1(\bar{r}) + (1 - \alpha) \sqrt{f_2(\bar{r})} \right] e^{i\bar{\theta}}, \\ A_1^{(1)}(\vec{x}, d, \alpha) &= - \left[\alpha \beta_1(\bar{r}) + (1 - \alpha) \beta_2(\bar{r}) \right] \frac{\sin \bar{\theta}}{\bar{r}}, \\ A_2^{(1)}(\vec{x}, d, \alpha) &= \left[\alpha \beta_1(\bar{r}) + (1 - \alpha) \beta_2(\bar{r}) \right] \frac{\cos \bar{\theta}}{\bar{r}}, \end{aligned} \quad (3.3)$$

where $\bar{r} = \sqrt{(x-d)^2 + y^2}$ and $\bar{\theta} = \arctan \frac{y}{x-d}$ are polar coordinates around the centre. Here, α is a free parameter whose value is chosen later. The desired $n = 2$ configuration can now be constructed using the standard superposition

$$\begin{aligned} \phi^{(2)}(\vec{x}, d, \alpha) &= \phi^{(1)}(\vec{x}, d, \alpha) \cdot \phi^{(1)}(\vec{x}, -d, \alpha), \\ A_k^{(2)}(\vec{x}, d, \alpha) &= A_k^{(1)}(\vec{x}, d, \alpha) + A_k^{(1)}(\vec{x}, -d, \alpha). \end{aligned} \quad (3.4)$$

Substituting this into (2.2) gives the energy

$$V(\alpha) = V[\phi^{(2)}(\vec{x}, d, \alpha), A^{(2)}(\vec{x}, d, \alpha)], \quad (3.5)$$

depending on α . Our numerical mesh ranges over the spatial rectangle $[-30, 30] \times [-15, 15]$, with $I_{\max} = 3201$ points in the x -component and $J_{\max} = 1601$ in the y -component. The mesh points are $\vec{p}_{ij} = (x_{\min} + i \delta x, y_{\min} + j \delta y)$ where $x_{\min} = -30$ and $y_{\min} = -15$, $\delta x = \delta y = 0.01875$

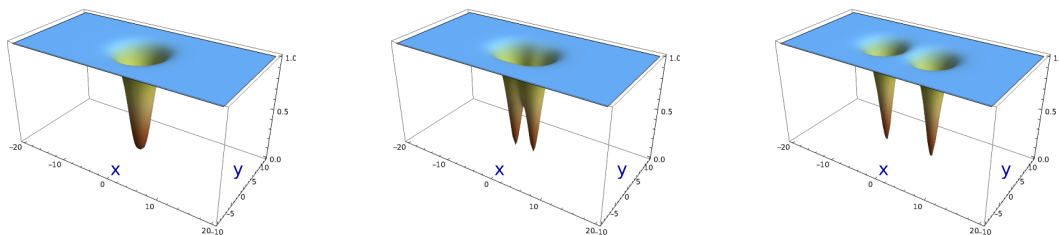


Figure 1. Potential wells $U = |\psi^{(2)}|^2$ of the 2-vortex fluctuation operator for $d = 0$ (left), $d = 2$ (middle) and $d = 5$ (right).

are the spatial steps, $i = 0, \dots, I_{\max} - 1$ and $j = 0, \dots, J_{\max} - 1$. A second-order finite difference scheme is employed to approximate the spatial derivatives arising in the functional energy (3.5). Now, for each d , the value of α is chosen to minimize (3.5). The analytical relation $\alpha = d^\epsilon / (d^\epsilon + \gamma)$ with $\epsilon = 3.4$ and $\gamma = 1.4$ is a good approximation. Finally, from this configuration, numerical gradient flow is employed to refine the solution. The resulting energies saturate the Bogomolny bound with a relative error less than 0.03%. These numerical 2-vortex solutions are precise enough to address the spectral problem of this paper. For later convenience, we denote their scalar field at the mesh points by $\psi^{(2)}(\vec{p}_{ij})$.

The next task involves the spatial discretization of the spectral problem (2.14) for $n = 2$, which will lead us to the positive discrete spectrum of the 2-vortex fluctuation operator \mathcal{H}^- , and hence \mathcal{H}^+ . Here, we can work with a less fine mesh than the previous one. We introduce new mesh points $\vec{q}_{ij} = (x_{\min} + i\Delta x, y_{\min} + j\Delta y)$ where Δx and Δy are the new spatial steps in each direction, $i = 0, \dots, i_{\max} - 1$ and $j = 0, \dots, j_{\max} - 1$. The fluctuation field values at the mesh points, $(a_1)_{ij} = a_1(\vec{q}_{ij})$, are arranged in a single column $(a_1)_s \equiv ((a_1)_{00} (a_1)_{01} \dots (a_1)_{0(j_{\max}-1)} (a_1)_{10} \dots (a_1)_{(i_{\max}-1)(j_{\max}-1)})^t$ where $s = j_{\max} \cdot i + j$, as also are the values of the background potential well,

$$U(\vec{q}_s) \equiv U(\vec{q}_{ij}) = |\psi^{(2)}(\vec{q}_{ij})|^2. \quad (3.6)$$

With this arrangement, the eigenvalue problem, discretized up to second order, is

$$-\frac{(a_1)_{s+j_{\max}} - 2(a_1)_s + (a_1)_{s-j_{\max}}}{(\Delta x)^2} - \frac{(a_1)_{s+1} - 2(a_1)_s + (a_1)_{s-1}}{(\Delta y)^2} + U(\vec{q}_s) (a_1)_s = \omega_\lambda^2 (a_1)_s. \quad (3.7)$$

Dirichlet boundary conditions have been assumed for the eigenfunctions, which implies that the value $(a_1)_s = 0$ is imposed for $s < 0$ and for $s \geq j_{\max} \cdot i_{\max}$. In addition, if $s \bmod j_{\max} = 0$ then $(a_1)_{[s/j_{\max}]j_{\max}-1} = 0$ where $[z]$ denotes the integer part of z , and likewise, $(a_1)_{[s/j_{\max}]j_{\max}} = 0$ for $s \bmod j_{\max} = j_{\max} - 1$. The procedure approximates the fluctuation operator by a finite matrix, which can be analysed to obtain the full spectrum of discrete eigenvalues and eigenfunctions. It has been checked that the choice $i_{\max} = 201$ and $j_{\max} = 101$ with $\Delta x = \Delta y = 0.3$, giving a fluctuation operator approximated by a 20301×20301 matrix, provides precise enough results. In figure 1, the potential wells $U(\vec{q}_s)$ of the discrete Schrödinger-type equation (3.7) are plotted for intervortex distance parameters $d = 0$, $d = 2$ and $d = 5$.

The main result of this paper is displayed in figure 2. This shows the three discrete positive eigenvalues ω_λ^2 , plotted as functions of d . To better understand the result we recall

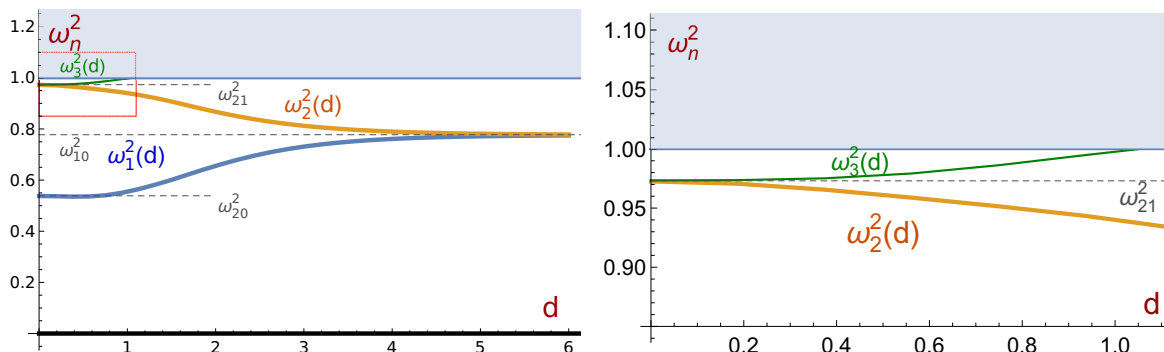


Figure 2. Eigenvalues of the 2-vortex fluctuation operator plotted against the intervortex separation parameter d (left). The red boxed area in the left figure has been enlarged on the right.

the spectrum of the fluctuation operator in the case of rotationally-invariant 1- and 2-vortices. Using the notation introduced in [2, 3], for the 1-vortex there is only one shape eigenmode with angular momentum number $k = 0$, eigenvalue $\omega_{10}^2 \approx 0.777476$ and eigenfunction $v_{10}(r)$. For the 2-vortex there is one eigenmode with angular momentum number $k = 0$, eigenvalue $\omega_{20}^2 \approx 0.53859$ and eigenfunction $v_{20}(r)$, and also a doubly-degenerate pair of eigenmodes with angular momentum number $k = 1$, eigenvalue $\omega_{21}^2 \approx 0.97303$ and eigenfunctions $v_{21}(r) \cos \theta$ and $v_{21}(r) \sin \theta$. The behaviour of the radial profiles $v_{10}(r)$, $v_{20}(r)$ and $v_{21}(r)$ is shown in refs. [2, 3]. We emphasize that the $k = 1$ mode is doubly degenerate when $d = 0$, because of the rotational invariance of the 2-vortex.

As the two vortices separate, the low-lying $k = 0$ eigenvalue $\omega_1^2(d)$ monotonically increases from the value $\omega_1^2(0) = \omega_{20}^2$ to $\omega_1^2(\infty) = \omega_{10}^2$, and the degeneracy of the next two eigenmodes is broken. The $k = 1$ eigenvalue splits into $\omega_2^2(d)$ and $\omega_3^2(d)$. The upper eigenvalue $\omega_3^2(d)$ increases from $\omega_3^2(0) = \omega_{21}^2$ as d increases, rapidly reaching the threshold of the continuous spectrum close to $d = 1$ where it disappears. On the other hand, $\omega_2^2(d)$ decreases from $\omega_2^2(0) = \omega_{21}^2$ and fuses with $\omega_1^2(d)$ around $d = 5$, where both approach ω_{10}^2 . More precisely, for two asymptotically-separated 1-vortices there are doubly-degenerate eigenmodes with eigenvalue $\omega_1^2(\infty) = \omega_2^2(\infty) = \omega_{10}^2$. These modes correspond to the symmetric and antisymmetric combinations of the localized, radial shape modes associated to the individual 1-vortices.

To emphasize this picture, in figure 3 the eigenmode a_1 of \mathcal{H}^- with eigenvalue $\omega_1^2(d)$ is plotted for selected values of d . We observe how starting at $d = 0$ from the $k = 0$ solution $a_1(r) = v_{20}(r)$, the eigenmode remains symmetric. Asymptotically, it may be understood as the symmetric linear combination of the 1-vortex modes, $a_1 \simeq v_{10}(\bar{r}_+) + v_{10}(\bar{r}_-)$ with $\bar{r}_\pm = \sqrt{(x \pm d)^2 + y^2}$. In figure 4 we plot the eigenmode with eigenvalue $\omega_2^2(d)$, starting from the $k = 1$ mode $a_1 = v_{21}(r) \cos \theta$ that is antisymmetric under $x \rightarrow -x$. The mode profile retains its antisymmetry as d grows. In particular, for large d , the mode becomes the antisymmetric linear combination of the 1-vortex modes, $a_1 \simeq v_{10}(\bar{r}_+) - v_{10}(\bar{r}_-)$.

The eigenmodes of the 2-vortex fluctuation operator \mathcal{H}^+ can be obtained from these eigenmodes of \mathcal{H}^- by using the intertwining formula (2.15). Since these are 4-component vectors, it is difficult to illustrate their precise form, or the way that they excite a 2-vortex solution. However, we can plot the potential energy density of an excited 2-vortex. Figure 5 shows snapshots of the oscillating 2-vortex solution at separation parameter $d = 1.5$, excited

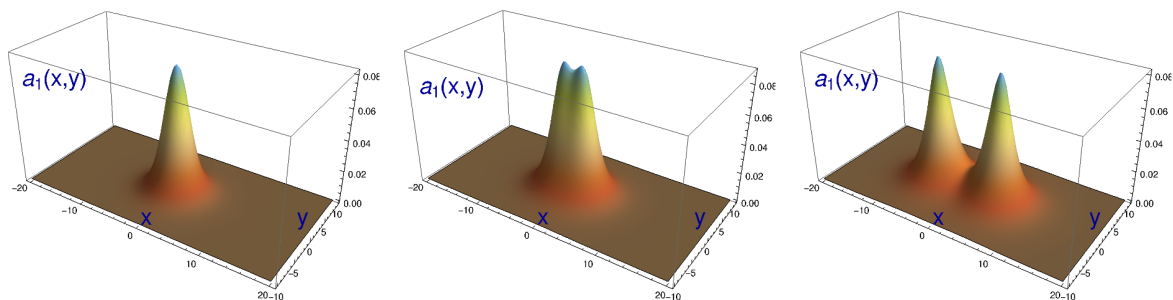


Figure 3. Eigenmode of the 2-vortex fluctuation operator with eigenvalue $\omega_1^2(d)$ for $d = 0$ (left), $d = 2$ (middle) and $d = 5$ (right).

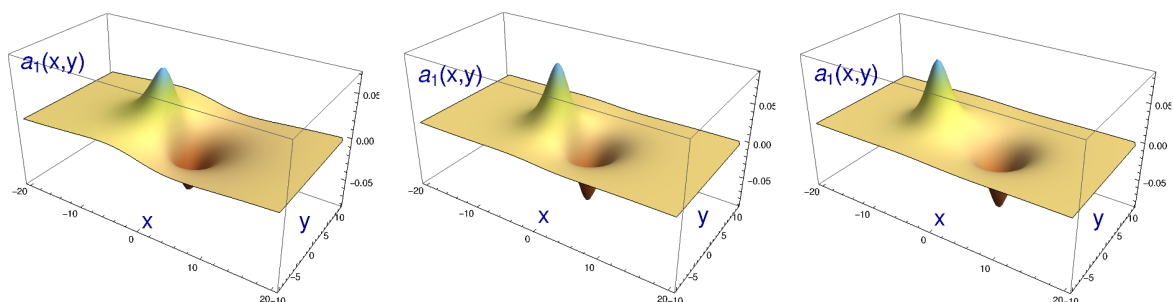


Figure 4. Eigenmode of the 2-vortex fluctuation operator with eigenvalue $\omega_2^2(d)$ for $d = 0$ (left), $d = 2$ (middle) and $d = 5$ (right).

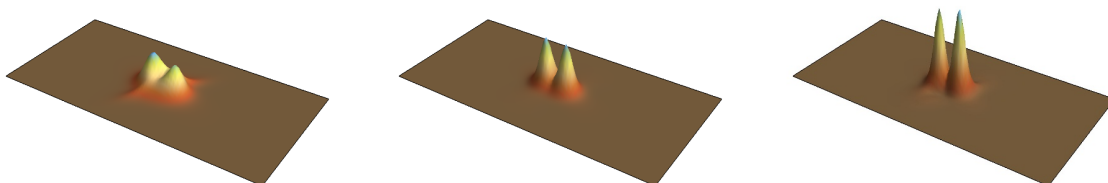


Figure 5. Snapshots of the oscillating 2-vortex at $d = 1.5$, excited by the mode of frequency ω_1 .

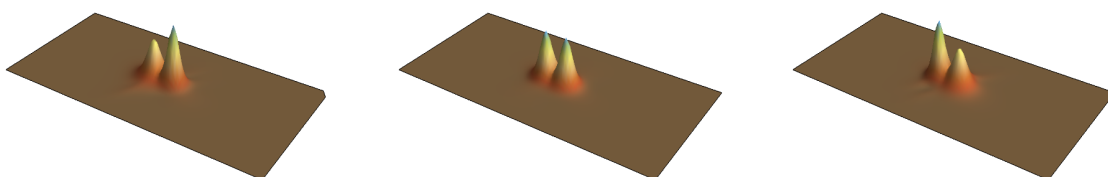


Figure 6. Snapshots of the oscillating 2-vortex at $d = 1.5$ excited by the mode of frequency ω_2 .

by the mode of lowest positive frequency, ω_1 . The constituent 1-vortices shrink and stretch in phase. Figure 6 shows the oscillations of the same 2-vortex excited by the discrete mode with the higher frequency, ω_2 . In this case, the 1-vortices oscillate in counterphase, i.e. while one vortex shrinks the other stretches.

4 Perturbation theory near $d = 0$

Here, we present some analytical calculations based on perturbation theory, that explain the spectral structure of the 2-vortex modes near the rotationally-invariant 2-vortex at $d = 0$. Specifically, we shall consider the eigenvalue problem (2.14) where the potential well is determined by the scalar part of a 2-vortex solution for small d , which we denote by

$$\tilde{\psi}^{(2)}(\vec{x}) = \psi^{(2)}(\vec{x}) + \epsilon \delta\psi^{(2)}(\vec{x}) + \dots . \quad (4.1)$$

$\psi^{(2)}(\vec{x})$ is the rotationally-invariant 2-vortex scalar field and $\delta\psi^{(2)}(\vec{x})$ is derived from the zero-frequency mode ξ_0 that splits the locations of the two overlapping 1-vortices, whose form is

$$\xi_0(\vec{x}) = \left(rh_{20}(r) \sin \theta, \quad rh_{20}(r) \cos \theta, \quad -\frac{rh'_{20}(r)}{f_2(r)}, \quad 0 \right)^t, \quad (4.2)$$

where $h_{20}(r)$ can be obtained numerically¹ (see section 4.1 in ref. [3]), and note that $h_{20}(r)$ is a decreasing function so $h'_{20}(r) < 0$. Therefore, the expansion (4.1) simplifies to

$$\tilde{\psi}^{(2)}(\vec{x}) = f_2(r)e^{2i\theta} - \epsilon \frac{rh'_{20}(r)}{f_2(r)} + \dots . \quad (4.3)$$

A relation between the perturbation parameter ϵ and the small distance parameter d can be derived from the zeros of (4.3). Near the origin, $f_2(r) \approx d_2 r^2$ and $h_{20}(r) \approx 1 + c_2^{(2,0)} r^2$ with $d_2 \approx 0.236146$ and $c_2^{(2,0)} \approx -0.277308$. Therefore

$$\epsilon = \frac{(d_2)^2}{2|c_2^{(2,0)}|} d^2 . \quad (4.4)$$

Notice that (4.3) is a first-order expansion in ϵ , so we are restricted here to a first-order treatment of the spectral problem (2.14). A higher-order expansion is a non-trivial task beyond the scope of this paper.

In addition to (4.1), the eigenmodes and eigenvalues must be expanded as

$$\begin{aligned} \tilde{a}_1(\vec{x}) &= a_1(\vec{x}) + \epsilon \delta a_1(\vec{x}) + \dots , \\ \tilde{\omega}^2 &= \omega^2 + \epsilon \delta \omega^2 + \dots , \end{aligned} \quad (4.5)$$

where $a_1(\vec{x})$ and ω^2 are a joint eigenmode and eigenvalue of the fluctuation operator \mathcal{H}^- associated to the rotationally-invariant 2-vortex, and ϵ is related to d as in (4.4). At first order, eq. (2.14) reduces to

$$\left[-\nabla^2 + |\psi^{(2)}(\vec{x})|^2 - \omega^2 \right] \delta a_1(\vec{x}) = \left(\delta \omega^2 - 2 \operatorname{Re}[\bar{\psi}^{(2)}(\vec{x}) \delta \psi^{(2)}(\vec{x})] \right) a_1(\vec{x}) . \quad (4.6)$$

From the Fredholm alternative it is known that the projection of the right-hand side of (4.6) on to the homogeneous solution (the eigenmode $a_1(\vec{x})$ at $d = 0$) must be zero in order to obtain bounded solutions. This implies that

$$\delta \omega^2 = \frac{\int d^2x \, 2 \operatorname{Re}[\bar{\psi}^{(2)}(\vec{x}) \delta \psi^{(2)}(\vec{x})] (a_1(\vec{x}))^2}{\int d^2x (a_1(\vec{x}))^2} . \quad (4.7)$$

We can now evaluate the integrals in (4.7) to estimate the three eigenvalues arising for small d .

¹Note, (4.2) separates the 1-vortices along the y -axis. Obviously, this has no essential consequence for the calculations shown here because of the rotational symmetry.

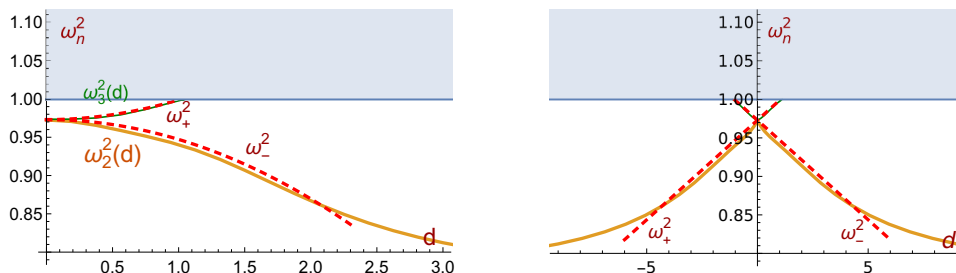


Figure 7. Comparison between the numerical results (solid) and first-order perturbative results for small d (dashed), for the eigenvalues ω_2^2 and ω_3^2 : (left) plotted against d , (right) plotted against $c = d^2$.

1. For the perturbed $k = 0$ mode at $d = 0$,

$$\delta\omega^2 = \frac{\int_0^\infty dr 2r^2 |h'_{20}(r)| v_{20}^2(r) \int_0^{2\pi} d\theta \cos 2\theta}{2\pi \int_0^\infty dr r v_{20}^2(r)} = 0 \quad (4.8)$$

because the angular integral vanishes. Therefore, the lowest non-degenerate eigenvalue has no quadratic dependence on d , so the leading dependence is quartic (at least), $\tilde{\omega}_1^2 = \omega_1^2 + O(d^4)$.

2. For the $k = 1$ mode proportional to $\cos \theta$ at $d = 0$,

$$\delta\omega^2 = \frac{\int_0^\infty dr 2r^2 |h'_{20}(r)| v_{21}^2(r) \int_0^{2\pi} d\theta \cos 2\theta \cos^2 \theta}{\int_0^\infty dr r v_{21}^2(r) \int_0^{2\pi} d\theta \cos^2 \theta} = \frac{\int_0^\infty dr r^2 |h'_{20}(r)| v_{21}^2(r)}{\int_0^\infty dr r v_{21}^2(r)} \approx 0.257323. \quad (4.9)$$

3. For the $k = 1$ mode proportional to $\sin \theta$ at $d = 0$,

$$\delta\omega^2 = \frac{\int_0^\infty dr 2r^2 |h'_{20}(r)| v_{21}^2(r) \int_0^{2\pi} d\theta \cos 2\theta \sin^2 \theta}{\int_0^\infty dr r v_{21}^2(r) \int_0^{2\pi} d\theta \sin^2 \theta} = -\frac{\int_0^\infty dr r^2 |h'_{20}(r)| v_{21}^2(r)}{\int_0^\infty dr r v_{21}^2(r)} \approx -0.257323. \quad (4.10)$$

Combining the last two results, we find the splitting of the eigenvalues ω_3^2 and ω_2^2 that are degenerate at $d = 0$,

$$\tilde{\omega}_{3,2}^2 \equiv \tilde{\omega}_\pm^2 \approx 0.97303 \pm \frac{(0.236146)^2}{2 \cdot 0.277308} 0.257323 d^2 \approx 0.97303 \pm 0.025873 d^2, \quad (4.11)$$

as shown in figure 7 (left). The similar dependence on d^2 , apart from the sign, is striking, and will be clarified in the next section.

5 Insight from the 2-vortex moduli space

The work of Taubes on BPS n -vortex solutions [6] and the later work of Samols on the Riemannian geometry of the n -vortex moduli space [7], reviewed in [8], make clear that it is best to set $z = x + iy$, and to use the complex variable $Z = X + iY$ to denote the location of a vortex (a zero of the scalar field), instead of the Cartesian 2-vector (X, Y) . An n -vortex solution is characterised by its n unordered zeros; good complex coordinates on the moduli

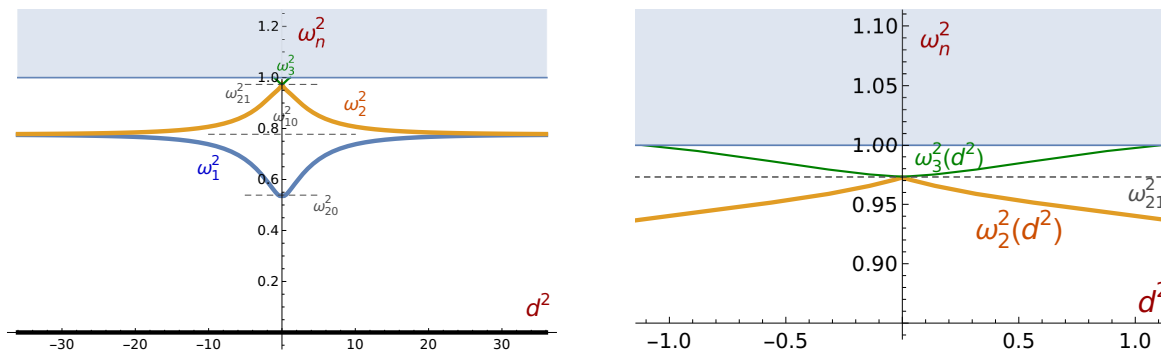


Figure 8. Dependence of the 2-vortex fluctuation operator eigenvalues on the parameter $c = d^2$ (left). The eigenvalue crossover region in the left figure has been enlarged on the right.

space are therefore the n elementary symmetric polynomials in these zeros. If the zeros are at $\{Z_1, Z_2, \dots, Z_n\}$, these coordinates are (up to sign) the coefficients of the polynomial

$$P(z) = (z - Z_1)(z - Z_2) \dots (z - Z_n). \tag{5.1}$$

Taubes showed that an n -vortex with these zeros exists and is unique up to gauge transformations, and in a convenient gauge has a scalar field ϕ that is a product of a real function with the polynomial $P(z)$.

For a 2-vortex with zeros at Z_1 and Z_2 ,

$$P(z) = z^2 - (Z_1 + Z_2)z + Z_1Z_2, \tag{5.2}$$

so good, 2-vortex moduli space coordinates are the centre of mass $\frac{1}{2}(Z_1 + Z_2)$ and the product $-Z_1Z_2$ (this sign choice is convenient). We are interested in vortices with centre of mass at the origin. In particular, if the vortices have Cartesian locations $(d, 0)$ and $(-d, 0)$, as above, then $Z_1 = d$ and $Z_2 = -d$, and the good coordinate for these centred vortices is $c = -Z_1Z_2 = d^2$. When $c = 0$, the vortices coincide at the origin, and the 2-vortex is rotationally invariant. Samols showed that the metric on the moduli space of centred 2-vortices has the form $ds^2 = F(|c|) dc d\bar{c}$, with F smooth and positive, including at $c = 0$.

There is a geodesic motion through moduli space, where c moves smoothly along the real axis from positive to negative values and the velocity of c remains negative throughout. What this means is that the vortices scatter through a right angle. If the vortices have Cartesian locations $(0, d)$ and $(0, -d)$, then $Z_1 = id$ and $Z_2 = -id$, so $c = -Z_1Z_2 = -d^2$. When c is positive, the vortex locations are on the x -axis; when c is negative, they are on the y -axis.

The eigenvalues and eigenmodes of the fluctuation operator around a 2-vortex are expected to flow smoothly over the moduli space. In particular, for centred vortices moving on the x -axis, the flow is smooth as a function of $c = d^2$. c is a better coordinate than d , and the flow remains smooth if the range of c is extended to negative values, corresponding to a right-angle scattering of the vortices. Furthermore, there is a symmetry between the vortex configuration with modulus c , and with modulus $-c$; they differ by a rotation through a right angle. So the eigenvalues of the discrete modes are the same at c and $-c$, and the eigenmodes should be related by a right-angle rotation.

The results we have obtained show that these expectations are fulfilled. The eigenvalues as a function of d (for $d \geq 0$) are shown in figure 2, but additionally, we have recalibrated the axes to show their dependence on $c = d^2$, and have reflected the graphs from right-to-left to show the eigenvalues for negative c . The outcome is figure 8. The same procedure has been applied to the perturbative results, as shown in figure 7 (right). The features to note in figures 2, 7 and 8 are (1) the graphs are smooth; (2) for small c , the dependence of the lowest eigenvalue ω_1^2 on c appears to be quadratic, as expected for a smooth symmetric function with a minimum. This quadratic dependence was verified through the perturbative analysis of section 4. It means that the dependence of ω_1^2 on d , shown in figure 2, is quartic, something that would be rather curious if one did not take into account the moduli space geometry; (3) the two eigenvalues ω_2^2 and ω_3^2 cross over smoothly and linearly at $c = 0$. This happens because for $c > 0$, the eigenmode for ω_2^2 is antisymmetric in x and symmetric in y , whereas for ω_3^2 it is the opposite way. As the vortices scatter through a right angle, the symmetry axes are exchanged, and the eigenvalues exchange their order. The linear dependence of these eigenvalues on $c = d^2$, and the smooth crossover, is verified by the formula (4.11) obtained through the perturbative analysis. In terms of d , the eigenvalues have quadratic dependence near $d = 0$, and crucially, the coefficients of the quadratic terms have opposite signs. The numerical results, shown in figure 7, do not exactly match these expectations. This could be because the numerical analysis is tricky for d very small, or it could be because the locations of the vortex zeros have moved slightly during the relaxation of the vortex configuration from the initial ansatz (3.4) to the optimised solution.

Recall that eigenvalue crossing is not generic as one parameter varies; instead the eigenvalues tend to repel and avoid crossing. However, here the crossing eigenvalues have eigenmodes with opposite symmetries, so there is no repulsion.

6 Outlook

We have obtained some detailed understanding of the discrete shape modes of BPS 2-vortex solutions, and how they vary with the separation of the 1-vortex constituents. It would be interesting to study the modification to the low-energy scattering of vortices when these modes are excited, either classically or quantum mechanically. The geodesic motion through the 2-vortex moduli space [7] will be supplemented by oscillation of the discrete modes and some potential energy function on the moduli space. An adiabatic treatment should be possible if the energy in the modes of oscillation is comparable with the kinetic energy of the translational motion of the vortices, and both are small. The simplest case would be when just one shape mode is excited. As the shape modes have different symmetries, the transfer of energy from one mode to another is likely to be suppressed. A complication may occur at the critical separation where one mode enters the continuum, should that mode be excited. We have seen that if vortices approach from a large distance, and their radial shape modes are excited in counterphase, then after they approach and scatter through a right angle, then it is this mode that enters the continuum.

A related program would be a search for fermionic bound states to vortices and an examination of their properties. This involves replacing Weinberg's first-order differential

operator by the Dirac operator, and investigating the spectral problem

$$\left\{ -i\gamma^j \left(\frac{\partial}{\partial x_j} - iV_j(x_1, x_2) \right) + 2|\psi(x_1, x_2)| \right\} \Psi(x_1, x_2; \omega) = \omega \Psi(x_1, x_2; \omega), \quad (6.1)$$

where $\gamma^0, \gamma^1, \gamma^2$ are 2×2 matrices that generate the Clifford Algebra of $\mathbb{R}^{1,2}$: $\{\gamma^\mu, \gamma^\nu\} = 2g^{\mu\nu}$. The 2-component spinors Ψ belong to the fundamental representation of the group $\mathbf{Spin}(2, 1; \mathbb{R})$, the component of the double cover of the Lorentz group $\mathbb{SO}(2, 1; \mathbb{R})$ connected to the identity. Its group elements and Lie algebra are given by

$$S(\omega_{\mu\nu}) = \exp \left[\frac{i}{2} \omega_{\mu\nu} \sigma^{\mu\nu} \right], \quad \omega_{\mu\nu} = -\omega_{\nu\mu}, \quad \sigma^{\mu\nu} = \frac{1}{2} [\gamma^\mu, \gamma^\nu]. \quad (6.2)$$

Finally, we mention that a similar analysis may be performed for the BPS vortices in the gauged massive non-linear sigma model, discussed in refs. [19–22] for example. Although such models are non-renormalizable, they may arise as low-energy effective theories within non-Abelian gauge theory or even string theory.

Acknowledgments

This work developed from a presentation at the SIG XI workshop, Jagiellonian University, Krakow. We thank A. Wereszczinski, K. Oles and C. Naya Rodriguez for organising the workshop.

This research was supported by the Spanish MCIN with funding from European Union NextGenerationEU (PRTRC17.I1) and Consejeria de Educacion from JCyL through the QCAYLE project, as well as the MCIN project PID2020-113406GB-I0. This research has made use of the high-performance computing resources of the Castilla y León Supercomputing Center (SCAYLE), financed by the European Regional Development Fund (ERDF). NSM is partially supported by consolidated grant ST/T000694/1 from the U.K. STFC.

Open Access. This article is distributed under the terms of the Creative Commons Attribution License ([CC-BY4.0](https://creativecommons.org/licenses/by/4.0/)), which permits any use, distribution and reproduction in any medium, provided the original author(s) and source are credited.

References

- [1] N.S. Manton, K. Olés, T. Romańczukiewicz and A. Wereszczyński, *Collective coordinate model of kink-antikink collisions in ϕ^4 theory*, *Phys. Rev. Lett.* **127** (2021) 071601 [[arXiv:2106.05153](https://arxiv.org/abs/2106.05153)] [[INSPIRE](#)].
- [2] A. Alonso-Izquierdo, W. Garcia Fuertes and J. Mateos Guilarte, *A note on BPS vortex bound states*, *Phys. Lett. B* **753** (2016) 29 [[arXiv:1509.06632](https://arxiv.org/abs/1509.06632)] [[INSPIRE](#)].
- [3] A. Alonso-Izquierdo, W. Garcia Fuertes and J. Mateos Guilarte, *Dissecting zero modes and bound states on BPS vortices in Ginzburg-Landau superconductors*, *JHEP* **05** (2016) 074 [[arXiv:1602.09084](https://arxiv.org/abs/1602.09084)] [[INSPIRE](#)].
- [4] M. Goodband and M. Hindmarsh, *Bound states and instabilities of vortices*, *Phys. Rev. D* **52** (1995) 4621 [[hep-ph/9503457](https://arxiv.org/abs/hep-ph/9503457)] [[INSPIRE](#)].

- [5] H. Arodz, *Bound states of the vector field with a vortex in the Abelian Higgs model*, *Acta Phys. Polon. B* **22** (1991) 511 [[INSPIRE](#)].
- [6] C.H. Taubes, *Arbitrary N : vortex solutions to the first order Landau-Ginzburg equations*, *Commun. Math. Phys.* **72** (1980) 277 [[INSPIRE](#)].
- [7] T.M. Samols, *Vortex scattering*, *Commun. Math. Phys.* **145** (1992) 149 [[INSPIRE](#)].
- [8] N.S. Manton and P. Sutcliffe, *Topological solitons*, Cambridge University Press, Cambridge, U.K. (2004) [[DOI:10.1017/CB09780511617034](#)] [[INSPIRE](#)].
- [9] E.B. Bogomolny, *Stability of classical solutions*, *Sov. J. Nucl. Phys.* **24** (1976) 449 [[INSPIRE](#)].
- [10] M.K. Prasad and C.M. Sommerfield, *An exact classical solution for the 't Hooft monopole and the Julia-Zee dyon*, *Phys. Rev. Lett.* **35** (1975) 760 [[INSPIRE](#)].
- [11] A.A. Abrikosov, *On the magnetic properties of superconductors of the second group*, *Sov. Phys. JETP* **5** (1957) 1174 [[INSPIRE](#)].
- [12] A. Alonso Izquierdo, W. Garcia Fuertes, M. de la Torre Mayado and J. Mateos Guilarte, *Quantum corrections to the mass of self-dual vortices*, *Phys. Rev. D* **70** (2004) 061702 [[hep-th/0406129](#)] [[INSPIRE](#)].
- [13] A. Alonso Izquierdo, W. Garcia Fuertes, M. de la Torre Mayado and J. Mateos Guilarte, *Quantum oscillations of self-dual Abrikosov-Nielsen-Olesen vortices*, *Phys. Rev. D* **71** (2005) 125010 [[hep-th/0504143](#)] [[INSPIRE](#)].
- [14] J. Mateos Guilarte et al., *Quantum fluctuations around low-dimensional topological defects*, *PoS ISFTG* (2009) 013 [[arXiv:0909.2107](#)] [[INSPIRE](#)].
- [15] E.J. Weinberg, *Multivortex solutions of the Ginzburg-Landau equations*, *Phys. Rev. D* **19** (1979) 3008 [[INSPIRE](#)].
- [16] P.J. Ruback, *Vortex string motion in the Abelian Higgs model*, *Nucl. Phys. B* **296** (1988) 669 [[INSPIRE](#)].
- [17] J. Burzlaff and D.H. Tchrakian, *Zero modes of rotationally symmetric generalized vortices and vortex scattering*, *J. Math. Phys.* **37** (1996) 650 [[hep-th/9507025](#)] [[INSPIRE](#)].
- [18] W. Garcia Fuertes and J. Mateos Guilarte, *Low-energy vortex dynamics in Abelian Higgs systems*, *Eur. Phys. J. C* **9** (1999) 535 [[hep-th/9812103](#)] [[INSPIRE](#)].
- [19] B.J. Schroers, *Bogomolny solitons in a gauged $O(3)$ sigma model*, *Phys. Lett. B* **356** (1995) 291 [[hep-th/9506004](#)] [[INSPIRE](#)].
- [20] M. Nitta and W. Vinci, *Decomposing instantons in two dimensions*, *J. Phys. A* **45** (2012) 175401 [[arXiv:1108.5742](#)] [[INSPIRE](#)].
- [21] A. Alonso-Izquierdo, W.G. Fuertes and J. Mateos Guilarte, *Two species of vortices in massive gauged non-linear sigma models*, *JHEP* **02** (2015) 139 [[arXiv:1409.8419](#)] [[INSPIRE](#)].
- [22] M. Speight and T. Winyard, *Intervortex forces in competing-order superconductors*, *Phys. Rev. B* **103** (2021) 014514 [[arXiv:2004.13171](#)] [[INSPIRE](#)].